

Adel M. Abdel Dayem^{1,*}

¹ Mechanical Power Engineering
Department, Faculty of Engineering,
Matarria, Helwan University,
Masaken El-Helmia, 11718 Cairo,
Egypt.

* Corresponding author. Email:
adel_abdeldayem@hotmail.com

Pioneer Solar Water Desalination System:

Experimental Testing and Numerical Simulation

Abstract: A pioneer system of solar water desalination was constructed, tested and numerically simulated for moderate latitudes, Cairo 30 °N. The humidification/dehumidification (HD) process is considered in this system. The salt water is heated by either solar energy or/and auxiliary heater before injection inside an insulated desalination chamber using an air atomizer. The air is supplied into a condenser by a 0.4 kW blower and later on it pulls hot salt water up through the atomizer from an insulated tank. By this idea the air is preheated inside the condenser and is used as a water pump. The flashing water is evaporated and condensed simultaneously above the condenser surface. A 2.39 m² flat-plate solar collector is used to heat the salt water existed in an insulated tank. The tank opening is closed by the chamber one. By this way the salt water is circulated naturally inside the solar water heater where it is forced inside the desalination chamber. A numerical simulation of the considered system was developed and validated. It was provided a mathematical model of each system component. The system was successfully tested using either solar or/and auxiliary energies. It can produce about 36 liter daily of purified water where the using of solar energy alone can obtain about 12 liter on clear days. To visualize the heat and mass transfer inside the chamber temperature and humidity distribution were measured. The annual and monthly performance of the system is presented. In addition an empirical equation of the distilled water quantity is obtained versus the incident solar radiation. Moreover, economic study was provided and it is found that one liter of distilled water can cost about 0.2 US\$ using the considered system.

Key words: Solar desalination; Air atomizer; Air condenser; Thermosiphon; Humidification/dehumidification; Numerical simulation

† Received 26 January 2011; accepted 22 February 2011.

Nomenclature

| | | | |
|-------------|--|-----------|---|
| A | Collector area, m ² | rc | Ratio of collector heat removal efficiency factor, FR, to the value at test conditions |
| A1-A6 | Variables of equation 23 | Re | Reynolds number for flow in pipes |
| Ac | Desalination chamber surface area, m ² | S | Total cost (fixed + operating) of the saline water supply per m ³ of product (≈ 0.03 US\$/m ³), |
| AP | Annual payment of the total capital investment as a percent of the investment per year | Ta | Ambient temperature, °C |
| Cp | Specific heat of working fluid, kJ/kg.K | Tc | Collector outlet temperature, °C |
| D | Diameter, m | Tci | Collector inlet temperature, °C |
| F | Friction factor | Tck | Temperature of kth node in collector, °C |
| F'UL | Product of the collector efficiency factor, F', and heat loss coefficient, UL, W/m ² .C | TD | Temperature of water delivered by tank to load, °C |
| FRUL | Slope of the collector efficiency versus (Tci - Ta)/IT curve, W/m ² .C | Th | Temperature of hot fluid entering tank, °C |
| FR | Intercept efficiency corrected for non-normal incidence | Ti | Temperature of ith segment, °C |
| g | Gravitational constant, m/s ² | TI | Effective annual tax and insurance charges as a percent of investment per year ($\approx 0.5\%$), |
| G | Collector flow rate per unit area, m ² | TI | Temperature of load stream entering tank, °C |
| Gtest | Collector flow rate per unit area at test conditions, kg/m ² | Tpi | Temperature of inlet fluid to pipe, °C |
| hfg | The latent heat of the distilled water at its temperature, kJ/kg | Tpo | Pipe outlet fluid temperature, °C |
| hL | Pressure head, m | TR | Temperature of fluid returns to heat source, °C |
| I | Total capital investment | Tsaline | Saline water temperature, °C |
| I | Storage tank segment | \dot{V} | Volume flow rate, m ³ /s |
| IT | Total incident radiation per unit area, W/m ² | Vh | Volume of fluid entering tank from heat source over a time interval t , m ³ /s |
| K | Friction factor of the piping connections | Vi | Volume of ith segment, m ³ |
| ks | Thermal conductivity | VL | Volume of fluid entering tank from load over a time interval t , m ³ /s |
| l | Length, m | Vt | Tank volume, m ³ |
| L | Annual operating man hours of hours of labor per year, | Uc | Desalination chamber heat loss coefficient, W/m ² .C |
| \dot{m} | Thermosiphon flow rate, kg/s | UA | Overall UA value of tank, W/C |
| \dot{m}_d | Distilled water mass flow rate, kg/s | W | Wage of the operating labor per man hour. |
| \dot{m}_h | Mass flow rate of hot stream entering tank, kg/s | Yd | Annual yield of distilled water, m ³ /year, |
| \dot{m}_L | Mass flow rate of load, kg/s | | Absorptance of the collector absorber |
| MR | Annual maintenance and repair (labor and materials) as percent of investment per year ($\approx 1\%$), | hi | Height of the ith node, m |
| N | Pay-out period (≈ 20 years), | Pi | Change in pressure across the ith node, N/m ² |
| Q_{in} | Rate of energy input to tank from hot fluid stream, W | ρ_i | Density of ith node, kg/m ³ |
| Q_{sup} | Rate of energy supplied to load by tank, W | | Density, kg/m ³ |
| Q_u | Rate of useful energy collection, W | | Transmittance of the collector glass covers |
| r | Annual fraction inflation rate (= 10% per year), | | |

Subscripts

| | | | |
|---|------------|---|----------------|
| A | Forced air | w | Flashing water |
|---|------------|---|----------------|

1. INTRODUCTION

The desalination process is provided by different methods, one of them is the evaporation/condensation (HD) process. In this method the salt water is evaporated and simultaneously condensed to produce distilled water. The HD process is based on the fact that air can be mixed with important quantities of vapor. The amount of vapor able to be carried by air increases with the temperature. In fact, 1 kg of dry air can carry 0.5 kg of vapor and about 670 kcal when its temperature increases from 30°C to 80°C. When an air flow is in contact with salt water, air extracts a certain quantity of vapor at the expense of sensitive heat of salt water, provoking cooling. On the other hand, the distilled water is recovered by maintaining humid air at contact with the cooling surface, causing the condensation of a part of vapor mixed with air. Generally the condensation occurs in another exchanger in which salt water is preheated by latent heat recovery. An external heat contribution is thus necessary to compensate for the sensitive heat loss.

Four parameters affect the evaporation process; a) air pressure, b) water temperature, c) water-air contact surface area and d) contact time of water with the surrounding air. Evacuation of the desalination unit can improve the evaporation rate but it is not so easy and it needs considerable awareness and limitations.

Of course the higher salt water temperature increases the water evaporation. The salt scaling problem can limit the allowable temperatures used. In addition, the temperatures at which the solar system can be efficiently used and the available waste heat must be taken in consideration.

The flashing-water contact surface area is increased by either increasing of flow rate or flashing the water into fine droplets. A limited decreasing of the droplets diameter improves the evaporation through improving of convective heat transfer of their surface. Moreover, using of forced air convection inside the desalination chamber may improve the evaporation rate as edited by Younis et al. (1993)^[1], Abdel-Salam (1993)^[2], Al-Hallaj et al. (1998)^[3] and Gao et al. (2008)^[4] at higher temperatures above 50 °C. Perhaps the natural convection is preferred as recommended by Farid et al. (1996)^[5], Nawayseh et al. (1997)^[6] and Mueller-Holst et al (1998)^[7] due to non-significant improvement if the forced circulation is considered as reported.

The contact time between the flashing water droplets and the surrounding air is based on the design of the desalination chamber. On the other hand, the heat convection is improved if the contact time of droplets with the surrounding air is enlarged. That can be provided by increasing the flashing path inside the desalination chamber. In all the above conducted systems and in the work of Abdel Dayem (2005)^[8], the hot salt water is injected vertically to down from the chamber roof. Therefore the contact time depends on the chamber height in this case.

For the solar energy as a heat source, the solar collectors are used to heat the salt water. The salt water can directly heated inside the collector as indicated by Gao et al. (2008)^[4], Abdel Dayem and Fatoh (2007)^[9], Nawayseh et al. (1999)^[10], Ben Bacha et al. (2003)^[11] and Nafey et al. (2004)^[12]. It was found a problem of salt scaling inside the solar collectors. That system is called open-loop system. The closed-loop system at which the salt water is heated indirectly along a heat exchanger between the collector and desalination loops. Such a system is used by Abdel Dayem, and Fatoh (2009)^[9] and Garg et al. (2002)^[13] indicating a little defect in the system performance. Accordingly a forced solar water heater was suggested by Abdel Dayem (2005)^[8], Ben Bacha et al. (2003)^[11] and Nafey et al. (2003)^[12]. Where the vacuum pressure is used inside the chamber it improves greatly the performance as indicated by Ahmad et al. (2009)^[14]. Moreover, more considered parameters and improvements can be found in Parekh et al. (2004)^[15]. On the other hand the cost of the water production can be reduced using different materials, flow rates and temperatures as indicated by Eslamimanesh and Hatamipour (2010)^[16].

In the present work, improving the desalination chamber performance is experimentally studied including the followings:

- i. injecting very fine water droplets using an air atomizer to improve the evaporation rate,
- ii. the hot water is ejected vertically to up to double the contact time between the droplets and the surrounded air,
- iii. using of preheated air to not lowering the droplets temperature,
- iv. the pumped air is used in the condenser as a condensation media and to pull up the salt water into the atomizer. In addition it improves the heat and mass transfer inside the desalination chamber.

In the previous work, the water is used as a condensation media and it is not edited any shortage in the condensation process. Therefore, study of using the air condenser may be efficiently considered.

In addition, an open-loop of a natural circulation (thermosiphon) solar water heater is considered in parallel with an auxiliary heater. The proposed system is installed and tested using either solar energy or auxiliary heater as a heat source. Moreover, a validated numerical simulation for the system is developed to study the system performance annually.

2. SYSTEM INSTALLATION, OPERATION AND MEASUREMENTS

The system consists of a solar water heater and desalination chamber those include:

Hot water tank – solar collector – blower – air distributor and atomizer– electrical heater and float – air condenser – connection pipes.

As explained above the salt water is heated in a 2.35 m² flat-plate solar collector to a 100-liter insulated galvanized steel tank. The flat-plate collector is tilted 30° and oriented to the south. The collector was tested using a local standard collector test rig at flow rate of 212.63 kg/h.m² and about 800 W/m² solar radiations. It is found that the collector efficiency curve has $F_R \tau \alpha = 0.5408$ and $F_R U_L = 2.0929$ W/m².C. On the tank upper opening, it is located an air atomizer to eject the hot salt water vertically up inside an insulated galvanized steel chamber. The chamber has dimensions of 1 x 1 x 1 m³ and is fixed carefully above the tank opening as shown in Fig. 1 and plate 1. A 0.4-kW centrifugal air blower, 380 volt, and about 65% efficiency supplies the air to the atomizer during the air distributor. The air is passed during a condenser to be preheated before going to the atomizer. As presented in Fig. 1, the condenser has a concave cross sectional area with a tapered bottom edge to collect the condensed water under the edge through an Aluminum channel tube to outside of the chamber. The 0.7 mm galvanized steel condenser consists of two containers 0.0405 m³ each connected in series. This idea lets the water injection with the vertical center-line of the chamber between the two containers. That obtains an uniform distribution of evaporation inside the chamber. And using of two containers condenser increases the condensing surface and improves the condensation variation. A strip is used under the condenser to prevent mixing of injecting salt water with condensed distilled water.

The system operation is simply achieved when the collector is considered to preheat the tank. The temperature is switched to about 70 °C by the auxiliary heater if used. This low temperature is considered to avoid the salt scaling which can partially close the atomizer holes. The condensed distilled water is collected under the condenser sides through channels to the outside of the system. The non-evaporated (saline) water is naturally going down to the tank by gravity. An amount of fresh water corresponding to the production rate is fed to the tank that is switched by a float.

The air distributor is simply constructed as shown in Fig. 1 from a stainless steel. It is a closed cylinder, its inlet is a tube that connecting to the condenser by a rubber hose. It has five outlets from its roof to allow the water/air droplet to go vertically up. Other five tubes that pulls up the water from the tank are fixed to the atomizer with five outlets. The distributor is fixed with the tank opening and immersed partially inside the water of the tank. The water level inside the tank is relatively constant because it is switched by the float.

By this design the desalination chamber and the heat source of hot water are compacted in one element. Thus eliminates the heat losses that are normally obtained during the water passes. An extra advantage is the elimination of heat losses from the return water passes. Although some of hot air is ventilated from the chamber through the clearance between the chamber walls and the tank opening those cause some heat losses but it improves the heat and mass transfer inside the chamber.

In solar-only mode where the solar energy is only considered, it is used to heat the tank water by few degrees. Perhaps it needs to leave the system one or two sunny days for the start up to raise the tank temperature. In that case the used temperature is not high but the system can work without any additional heat. In solar/auxiliary mode, two-kW auxiliary electrical heater raises the tank temperature into the switched one, 70 °C. The heater is fixed inside the upper third of the tank. It can keep a relatively constant temperature during the operation.

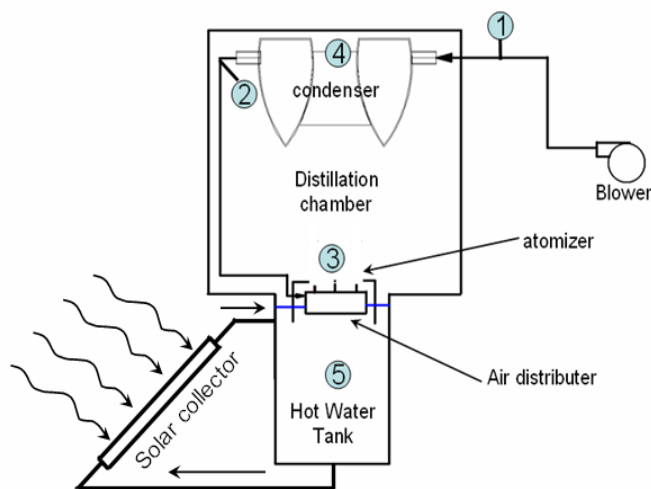


Fig. 1: Schematic diagram of the considered system

Plate 1: Photograph of the desalination unit

To present the temperature variation inside the desalination chamber k-type thermocouples are distributed during it to monitor all of chamber enclosure. They are connected to the digital dual input thermometer (type K). It is of type BK Precision (model 710). In addition, the moisture inside the chamber is measured by a thermo Hygrometer. The thermocouples were calibrated and tested to estimate the correct measured temperatures. Moreover, the salinity of water is measured by a salinity meter with resolution of 0.01 where the pressure is simply measured by a Bourdon gauge and a flow meter is used to measure the air flow rate. Moreover a thermometer is used to measure the exit and inlet temperatures of the water and air.

The system operation can be summarized as presented in Fig. 1 as the followings:

- i. The blower delivers fresh air (point (1)) into the air condenser to be preheated at points (2) and (4).
- ii. The exit air from the condenser enters the air distributor in order to pull up the hot water through the atomizers making a vacuum pressure (point (3)).
- iii. The water is flashed by the air inside the desalination chamber through four atomizers. The atomizer used has one air nozzle with diameter 3mm and one water pipe with diameter 4mm, the air nozzle is perpendicular to the water pipe.
- iv. The atomizers (are used as an evaporator) humidifies the air inside the desalination chamber. Due to density difference, the humid air moves up towards the cold surface of the condenser. It is condensed on the condenser surfaces and collected later to outside the chamber.

- v. The saline water that did not evaporate returned to the cycle by gravity force to the hot water tank (saline water tank, 5)

3. MATHEMATICAL MODEL OF THE SYSTEM

The system consists of a thermosiphon solar water heater and a desalination chamber. Therefore it is shown the mathematical model of each part.

3.1 Thermosiphon Solar Water Heater

As described in the manual of the TRNSYS software [17] the thermosiphon system consists of a flat-plate solar collector, a stratified storage tank, a check valve to prevent reverse flow, and water as the working fluid as shown in Fig. 1 and Plate 1. Flow in the loop is assumed to be steady-state. The system is analyzed by dividing the thermosiphon loop into a number of segments normal to the flow direction and applying Bernoulli's equation for incompressible flow to each segment. The flow rate is obtained by numerical solution of the resulting set of equations.

Application of Bernoulli's equation to any node, i , in the thermosiphon loop results in the following expression for pressure drop.

$$\Delta P_i = \rho_i \cdot g \cdot \Delta h_i + \rho_i \cdot g \cdot h_{Li} \quad (1)$$

The thermosiphon model involves the numerical solution for the flow rate that satisfies the above equation. The density of the fluid is evaluated at the local temperature using a correlation for water. Temperatures and frictional head losses in each node of the collector and pipes are determined as described below. The collector inlet and outlet pipes are each considered to be single nodes, with negligible thermal capacitance.

A first law analysis yields the following expressions for average and outlet temperatures of these pipes.

$$T_{po} = T_a + (T_{pi} - T_a) \exp \left[-\frac{(UA)_p}{mC_p} \right] \quad (2)$$

Frictional head loss in either pipe is given as

$$H_p = \frac{f \cdot L \cdot v^2}{2d} + \frac{Kv^2}{2} \quad (3)$$

where K is the friction factor for the piping connections and the friction factor, f , is

$$f = \frac{64}{Re} \quad \text{for } Re < 2000$$

$$f = .032 \quad \text{for } Re > 2000$$

By this way the pressure drop can be estimated through the pipes and collector risers and headers where the friction head loss in the tank is neglected.

The net weight of fluid in the collector is found by dividing the collector into N_x equally sized nodes. The thermal performance is modeled according to the Hottel-Whillier equation. The temperature at the midpoint of any collector node, k , is

$$T_{ck} = T_a + \frac{I_T F_R (\tau \alpha)}{F_R U_L} + \left(-T_a - \frac{I_T F_R (\tau \alpha)}{F_R U_L} \right) \cdot \exp \left[\frac{\hat{F} U_L}{G \cdot C_p} \cdot \frac{(k - \frac{1}{2})}{N_x} \right] \quad (4)$$

The collector parameter $\hat{F} U_L$ is calculated from the value of $F_R U_L$ and G at test conditions

$$\hat{F} U_L = -G_{test} \cdot C_p \ln \left(1 - \frac{F_R U_L}{G_{test} C_p} \right) \quad (5)$$

The overall useful energy collection is:

$$Q_u = r_c A (F_R(\tau\alpha) I_T - F_R U_L (T_{ci} - T_a)) \quad (6)$$

where

$$r_c = \frac{F_R |_{use}}{F_R |_{test}} = \frac{G(1 - \exp(-\frac{\dot{F}U_L}{GC_P}))}{G_{test}(1 - \exp(-\frac{\dot{F}U_L}{G_{test}C_P}))} \quad (7)$$

The Tank

The tank is initially divided into four segments of volume V_i and temperature T_i , so that no temperature inversions are present. In one time period, the heat source delivers a volume of liquid, V_h , equal to $\dot{m}_h \Delta t / \rho$ at a temperature T_h . Assuming T_h is greater than T_1 (first segment temperature), then a new segment is added at the top of the tank and the existing profile is shifted. At the same time, the fluid enters from the load with a volume, V_L , equal to $\dot{m}_L \Delta t / \rho$ and temperature of T_L . If T_L is less than T_4 (fourth segment temperature), then a segment is added at the bottom of the tank and the profile is shifted once more. The net shift of the profile in the tank is equal to the difference between the total heat source volume and load volume or $(\dot{m}_h - \dot{m}_L) \Delta t / \rho$.

The average temperature delivered to load is:

$$T_D = \frac{V_h T_h + (V_L - V_h) T_1}{V_L} \quad (8)$$

Storage losses from the tank and conduction between segments are evaluated before the temperature profile has been adjusted for flows. This is accomplished by solving the following differential equation for each segment:

$$\rho C_P V_i \frac{dT_i}{dt} = -(UA)_i (T_i - T_{env}) + (k_s A)_{i-1} \frac{(T_{i-1} - T_i)}{\Delta h_{i-1}} - (k_s A)_i \frac{(T_i - T_{i+1})}{\Delta h_{i+1}} \quad (9)$$

where Δh_{i-1} = separation between centers of segments $i-1$ and i , and Δh_{i+1} = separation between centers of segments i and $i+1$.

The energy input to the tank due to the hot inlet stream is

$$Q_{in} = \dot{m}_h C_P (T_h - T_R) \quad (10)$$

The energy supplied to the load is

$$Q_{sup} = \dot{m}_L C_P (T_D - T_L) \quad (11)$$

3.2 Desalination Chamber

To simulate the desalination chamber the atomized water flow rate is required. To estimate it the Bernoulli equation for incompressible flow is applied between the points 1, and 2 and between 3 and 2 as shown in Fig. 2. First the air flow rate (\dot{V}_a) can be estimated from the blower power as:

$$\dot{V}_a = P_f \eta_f / (g * H_a * \rho_a) \quad (12)$$

Applying Bernoulli equation between the points 1 and 2 for water flow gets.

$$h_{LW} = \left[\frac{f_W L_W}{D_2} + 1.2 \right] \frac{8 \dot{V}_W^2}{\pi^2 g D_2^4} \quad (13)$$

Similarly applying Bernoulli equation between the points 3 and 2 for water flow gets.

$$h_{La} = \left[\frac{f_a L_a}{D_3} + 1.2 \right] \frac{8 \dot{V}_a^2}{\pi^2 g D_3^4} \quad (14)$$

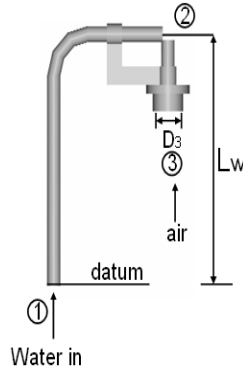


Fig. 2: Schematic diagram of the atomizer and air distributor

$$\text{And } h_L = \frac{0.2}{g\rho_a} \quad (15)$$

So the atomized water flow rate can be determined as:

$$\dot{V}_W = 4 \sqrt{\frac{-h_L + h_{Lw} + \dot{V}_a^2}{h_{Lw}}} \quad (16)$$

To estimate the distilled mass flow rate, an energy balance is applied for the desalination chamber as the input energy to the chamber (input atomized water and air, and inlet air) equals the output energy (output distilled water, and saline water and outlet air), the equation (3) is developed.

$$A1 = C_p(T_d - \frac{T_a}{2} - \frac{T_D}{2}) \quad (17)$$

$$A2 = \rho_W \dot{V}_W C_p T_D \quad (18)$$

$$A3 = \rho_a \dot{V}_a C_{pa} T_a \quad (19)$$

$$A4 = \rho_a \dot{V}_a C_{pa} (T_a + T_D)/2 \quad (20)$$

$$A5 = U_c A_c [(T_a + T_D)/2 - T_a] \quad (21)$$

$$A6 = \rho_W \dot{V}_W C_p (T_a + T_D)/2 \quad (22)$$

$$m_d = (A2 + A3 - A4 - A5 - A6)/A1 \quad (23)$$

Assume that the distilled outlet water temperature, $T_d = T_D - 8$ and the saline water outlet temperature,

$$T_{\text{saline}} = (T_D + T_a)/2 \text{ and } T_{ao} = \left[\frac{m_d h_{fg}}{\rho_a \dot{V}_a C_{pa}} \right] + T_a.$$

The above 23 equations are solved simultaneously together for each time step to estimate the different variables considered under the measured weather data of Cairo city.

4. RESULTS AND DISCUSSION

4.1 Experimental Performance of the System

The installed system was experimentally tested and the following scenarios were considered.

4.1.1 Constant Temperature System

In this system the auxiliary heater is used to heat up the salt water in the tank into specified temperature. That was provided to study the performance of the system under relatively constant conditions. The performance of the desalination unit is evaluated by the quantity of the distilled water produced. The measured data is observed as follows:

- At start, fresh air temperature entering condenser is about 30 °C.
- During operation, condensers exit-cooling air reaches 50°C (at warm up) to 55 °C (at steady state) with a regular volume flow rate of 0.085 m³/s.

- Pressure air distributor is about 1.2 bar.
- Hot water feeding the atomizer (humidifier) is about 70 °C.
- Exit desalinate water temperature is about 30 °C.
- Relative humidity (RH) in the side of the condensers enclosure is measured between 18 % (at warm up) to 30% (at steady state) and in the side of the humidifier enclosure; it ranges between 60 to 80%.
- After 15 minutes of operation, the steam was condensed and collected in the channel. This delay can be considered as the warm up period of the desalination unit.
- Desalinate water was collected in a beaker; it was found that 1.5 liter was collected each hour. It can produce about 36 liter/day if it works continuously 24 hours.

The temperature distribution inside the desalination chamber was obtained by measuring the temperatures at different locations inside it as shown in Fig. 3. By these points the chamber was divided into 48 parts. Then twenty seven locations are distributed regularly along the desalination chamber to visualize the temperature and relative humidity variation. So the temperatures were measured in two levels that distant 25 and 75 cm from the chamber floor simultaneously. In each location a thermocouple is fixed to measure the temperature in it. The temperature distribution is indicated in Fig. 4 for each position explained. A little difference is found between different locations. That explains that the temperature is good distributed along the chamber. That is obtained from the similarity of the chamber components. The maximum temperatures are obtained along the center-line region and that are accepted from the heat transfer point of view. As shown in the figure the temperature variation at the same plane is not homogeneous due to inhomogeneous heat losses from the desalination chamber. In addition, the room enclosure surrounded the second condenser part from the air inlet is little heated due to warm air inside it that was preheated inside the first part.

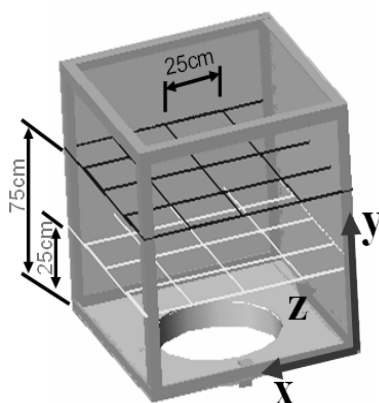


Fig. 3: Locations of the measurements inside the desalination chamber

To study the performance of the condenser and evaporator, the temperature was measured for each side (an average value). A lower value of temperature of the condenser side indicates that the condenser surfaces are big enough to condensate all of evaporated steam. That can be seen in the form of low humidity measured as shown in Fig. 5. Therefore the flow rate of the evaporated hot water could be raised. That is clearly presented in Fig. 6 at which the high air flow rate increases linearly the distilled water quantity.

As expected, the enclosure that surrounds the condenser has the minimum relative humidity. The vapor is condensed on the condensers surfaces. In the far regions the vapor is increased causes higher relative humidity. It exchanges the mass and heat with the near regions of condenser naturally. As shown in Fig. 5 the maximum relative humidity is about 80%, it is not saturated yet. Therefore, considering forced heat and mass transfer inside the desalination chamber is successfully provided. In addition, the quantity of distilled water is relatively constant after the warming up process, after about fifteen minutes.

In fact, increasing water flow rate increases heat and mass transfer coefficients as well as the solar collector efficiency. At the same time, it lowers the operating water temperature in the unit and hence, lowers the evaporation and condensation rate. The optimum flow rate is significantly affected by the desalination unit size, evaporative area and condenser surface area. As presented in Fig. 6, a linear relation between the air flow rate and the quantity of produced distilled water is found. The optimum flow rate could be determined based on an economical study.

According to that, it was shown that the mass of the unit is other factor that badly affects the unit performance. A delay of 15 minutes was recorded before the steady production of fresh water. It was noticed that most of the energy received in these early minutes is used as sensible heat to warm up the large mass of the unit, which is about 150 kg. This lag time could be avoided by using a lighter material than galvanized steel for construction.

The influence of feeding hot water on the unit productivity with natural air circulation shows that increasing the temperature of feeding water increase the productivity, while the ambient temperature has a negligible effect on the total productivity, that is accepted with the results of Parekh et al.^[15]. On the other hand, increasing the evaporating salt water may raise the possibility of scales concentration.

In Fig. 5 the relative humidity distribution inside the desalination chamber is presented. It is drawn as contours in three levels along the chamber height. The chamber door is located at the plane of Z=0. As described in the figure, the middle level has the highest humid air. That can be expected because that level is located far from the condenser and atomizer. Moreover the moist area of this level (about 75%) is located in the side of air inlet to the chamber that is colder than the other sides.

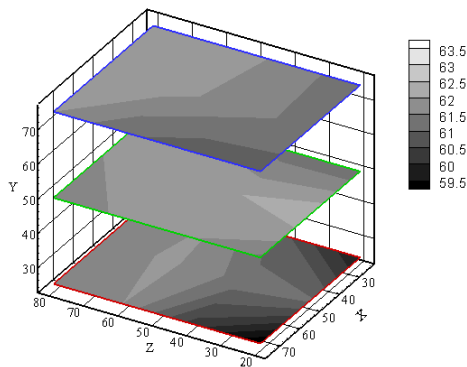


Fig. 4: Temperature distribution inside the desalination chamber for constant heating temperature

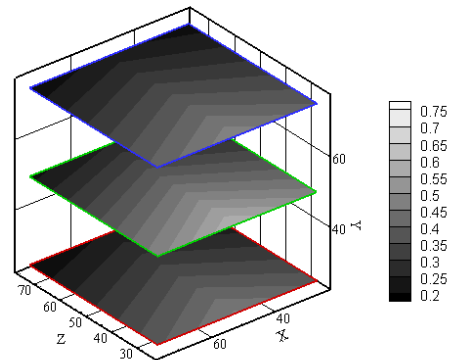


Fig. 5: Relative humidity distribution inside the desalination chamber for the constant heating temperature system

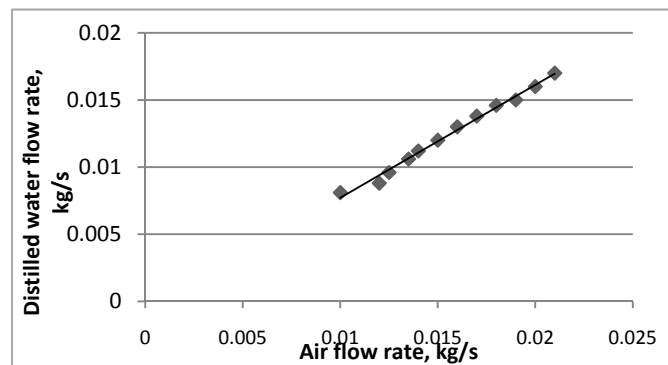


Fig. 6: Relation of produced distilled water versus the air flow rate

The other two levels have the same variation of relative humidity with higher values. The variation is regular around the regular shape condenser from right to left of Fig. 5. Also the relative humidity is linearly varied from front to back of the chamber. That is due to regular raise in the air temperature inside the condenser.

4.1.2 Solar-alone System

The system is tested for the solar energy as a unique heat source. If the solar energy is only used as a heat source, lower temperatures are obtained as presented in Fig. 7. Lower temperatures than the first case are obtained due to lower heating temperature. That is seen in low productivity in that case and is clearly affected by the condenser location. The temperature distribution inside the chamber is slightly changed from the first case. That can be understood as a result of using lower temperature of evaporation. That temperatures are normally changed from time to time based on the incident solar radiation and ambient temperature. As expected the upper plane of temperatures' locations has the highest temperatures. The significant effect of using air condenser is clearly presented in form of air temperature along the chamber, where the temperature is low in the inlet air side it raises in the exit side. That affects the condensation process, it increases in the cold side while it decreases in the hot one.

Accordingly the upper level has the higher temperatures while the lower level has the lower ones. Moreover, it is found that the system in that case can produce about 10 liters of desalinate water a daytime as shown in Fig. 8. That quantity depends basically on the used solar collector efficiency which is relatively low in this work. If an efficient collector is used the system output can be improved. Concerning the quality of water, we notice that in comparison with the other desalination installations functioning with extraction of non-condensable gases, the distilled water produced in the HD installations is saturated with oxygen. In this case, it is sufficient to add active carbon and dolomite to improve the taste.

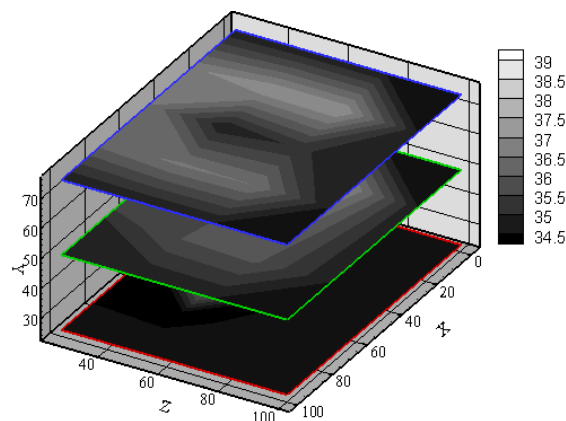


Fig. 7: Temperature distribution inside the desalination chamber if the solar energy source is only used

4.2 Validation of the Numerical Simulation and Annual Performance of the System

The installed system with the same specifications, geometry and dimensions is considered in the numerical simulation. To validate the numerical simulation the program was running under the same weather conditions of the experimental data that are shown in Fig. 9. As indicated in Fig. 8 the hourly produced distilled water is compared for the simulated and measured values. The daily accumulated of the distilled water is also indicated for the simulation and experimental conditions. The estimated hourly variation of the distilled water is in close agreement with the measured ones. The difference between them is about 10%. That difference is due to some factors not considered in the numerical simulation. Those factors are (a) the heat stored in the system materials, (b) the transmittance variation of the collector glass, (c) the atomized water temperature that was considered as the

average temperature, (d) the outlet air and distilled water temperature were taken as average values, (e) the assumptions those were considered for the energy equation to estimate the atomized water quantity.

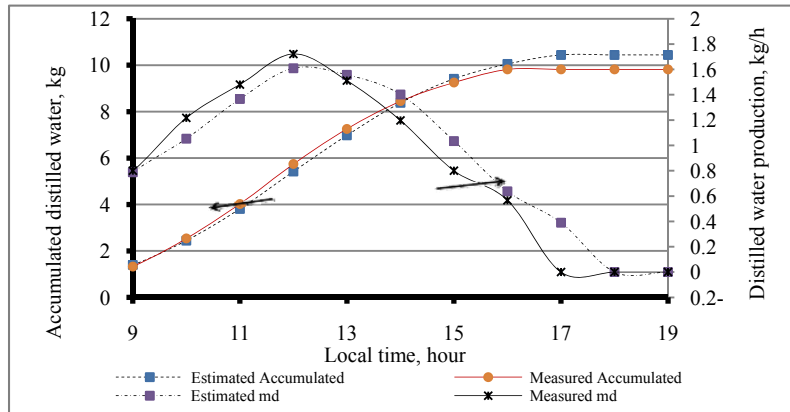


Fig. 8: Comparison between the simulated and measured distilled water production of the considered system

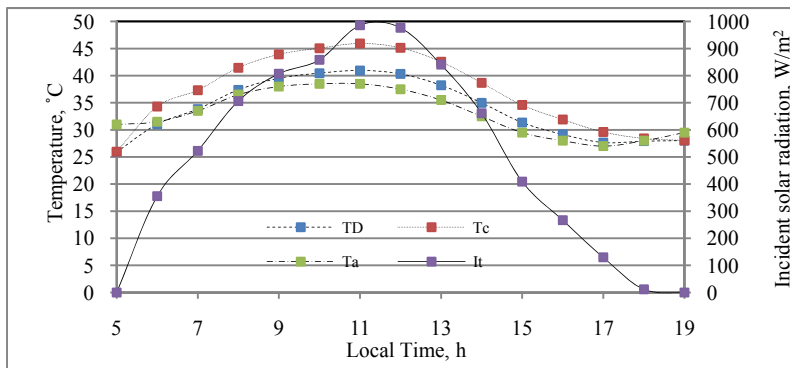


Fig. 9: Temperatures and incident solar radiation on the day of comparison

In general the difference in the hourly variation between the estimated and measured values makes no significant difference in the accumulated values and the validation can be accepted. On the other hand the hourly variation in the collector outlet temperature (T_c) and load temperature (T_L) to the atomizer are shown in Fig. 9. Its variation is similar to the solar radiation variation as expected. Perhaps the temperatures are not high due to utilizing the hot water from tank continually although the ambient temperature is not low.

The annual variation of the produced distilled water is presented in Fig. 10. It shows the hourly values along the year. As expected the quantity of distilled water is maximized during the summer season and is minimized during the winter months. The annual variation of the distilled water is very close to the annual variation of the solar radiation and ambient temperature. The ambient temperature has not higher effect on the system performance. The water production ranges from about 0.5 kg/h to about 1.8 kg/h. The annual production of the system is about 2833 liters. The figure presents also the temperature variation of the distilled water, It is similar to the water production variation. Perhaps the temperature is relatively high (about 28 °C) in the summer but it can be accepted relative to the ambient temperature in that period of time.

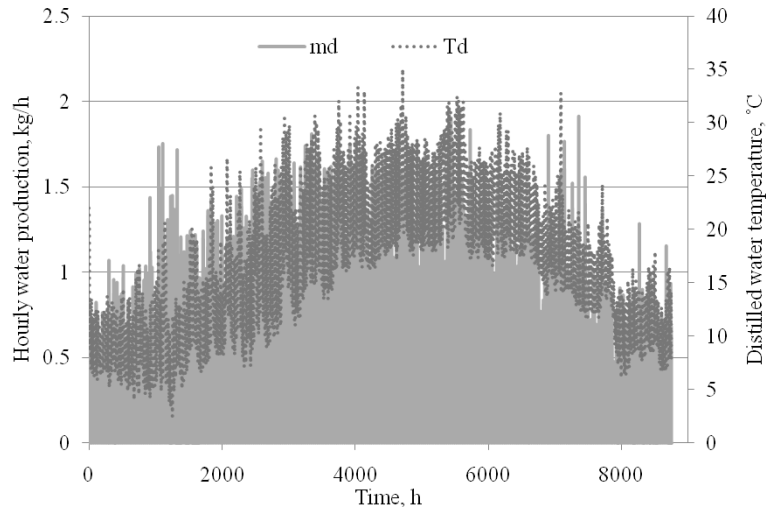


Fig. 10: Annual variation of distilled water production and temperature

The monthly average quantity of the distilled water is estimated in Fig. 11. The months of May to August have the highest production along the year where December and January have the lowest values as expected. The average yearly values can be found during the months March, April, October and November.

The system efficiency is estimated annually under the weather conditions of Cairo °N. The system efficiency is defined as:

$$\eta = \frac{m_a h_{fg}}{I_T \cdot A} \tag{24}$$

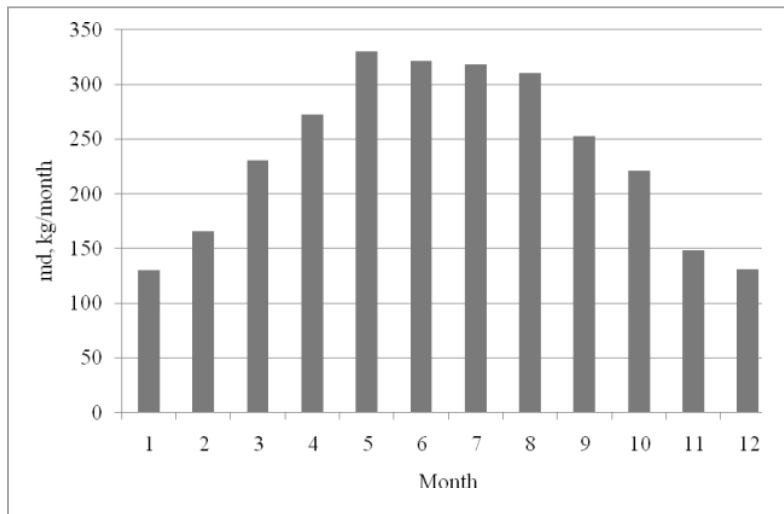


Fig. 11: Monthly production of the distilled water

In Fig. 12 the annual variation of the system efficiency is presented. The system efficiency is changed from day to day depending on the input solar radiation and ambient temperature. Therefore it has no defined trend along the year and it has no seasonal performance. Its average value is not widely improved during the summer months due to higher ambient temperature. That can be understood because the ambient temperature has no higher significance on the system performance.

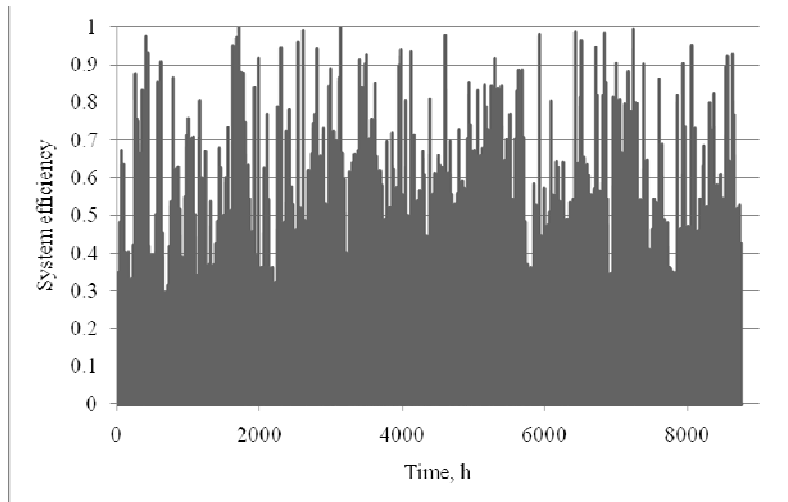


Fig. 12: Annual variation of the system efficiency

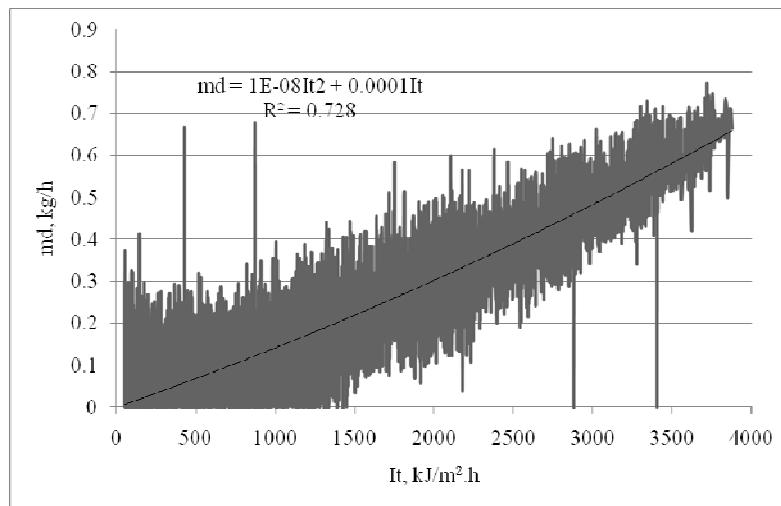


Fig. 13: Water production versus the incident solar radiation

In Fig. 13 the distilled water mass flow rate (kg/h) is estimated versus the total incident solar radiation (kJ/m².h) on the collector during a year. The data is fitted as a second order equation with about 27 % error. From that equation m_d can be determined for any input value of solar radiation. The equation is obtained as:

$$m_d = 10^{-8}I_T^2 + 0.0001I_T \quad (25)$$

4.3 Economics of the Desalination System

The cost of water production per cubic meter of desalinate, C, can be estimated as edited by Elsayed et al. [18]

$$C = \frac{I(AP + MR + TI) + L.W}{Yd} + S \quad (25)$$

Where $AP = r \left[1 + \frac{1}{(1+r)^n - 1} \right]$ (26)

The initial (capital) cost of the system is about US\$ 500. If the annual operating man hours is 500 hours at a wage of \$ 5/hr and the average annual productivity of about 13 m³. Then estimating the liter cost of the distilled

water is about 0.2 US\$/liter. Probably it is higher than that produced by the conventional energy as concluded by El-Nashar (2001) [19] but it is sometimes in urgent needs.

5. CONCLUSION

An efficient humidification-dehumidification solar desalination system was designed, installed and tested at solar energy laboratory, Mattarria faculty of Engineering, Cairo, Egypt. The system can work by either solar energy or auxiliary heater or both. A natural-circulation solar water heater is used as a heat source. A forced air is used as a condenser fluid and later on it is used as an atomizer of hot salt water. The system can work continuously and the daily productivity of the distilled water is about 36 l/day. That is corresponding to 0.37 liter for each kilowatt-hour of input energy. When the system uses solar energy only it can produce about 5 l/m² d. That can be accepted according to previous conducted work. A validated numerical simulation of the system was developed. The predicted results are in close to the measured ones. The system performance was presented annually and monthly. An empirical equation of the produced distilled water was obtained. The price of clean water can cost about 0.2 US\$/liter. From the system testing it was found that using forced air system increases water atomization and making good condensation.

REFERENCES

- [1] Younis, M. A., Darwish, M. A., Juwayhel, F. (1993). Experimental and theoretical study of a humidification-dehumidification desalting system. *Desalination*, 94, 11-24.
- [2] Abdel-Salam, M. S., Hilal, M. M., El-Dib, A. F., Abdel, Monem M. (1993). Experimental study of humidification-dehumidification desalination system. *Energy Sources*, 15, 475-490.
- [3] Al-Hallaj, S., Farid, M. M., Tamimi, A. (1998). Solar desalination with a humidification--dehumidification cycle: performance of the unit. *Desalination*, 120, 273-280.
- [4] Gao, P., Zhang, L., Zhang, H. (2008). Pump with humidification and dehumidification performance analysis of a new type desalination unit of heat. *Desalination*, 220, 531-537.
- [5] Farid, M., Al-Hajaj, A. (1996). Solar desalination with a humidification-dehumidification cycle. *Desalination* 106, 427-429.
- [6] Nawayseh, K. N., Farid, M. M., Omar, A., Al-Hallaj, S., Tamimi, A. (1997). A simulation study to improve the performance of a solar humidification-dehumidification desalination unit constructed in Jordan. *Desalination*, 109, 277-284.
- [7] Mueller-Holst, H., Engelhardt, M., Herve, M., Scholkopf, W. (1998). Solar thermal seawater desalination systems for decentralized use. *Renewable Energy*, 14(1-4), 311-318.
- [8] Abdel, Dayem A. (2006). Experimental and numerical performance of a multi-effect condensation–evaporation solar water distillation system. *Energy*, 31, 2374-2391.
- [9] Abdel, Dayem A. M., Fatoh, M. (2009). Experimental and numerical investigation of humidification/ dehumidification solar water desalination systems. *Desalination*, 247, 594–609.
- [10] Nawayseh, K. N., Farid, M. M., Omar, A., Sabirin, A. (1999). Solar desalination based on humidification process-II, computer simulation. *Energy Conversion & Management*, 40, 1441-1461.
- [11] Ben, Bacha H., Damak, T., Bouzguendra, M., Maalej, A. Y. (2003). Experimental validation of the distillation module of a desalination station using the SMCEC principle. *Renewable Energy*, 28, 2335–2354.
- [12] Nafey, S., Fath, H. S., El-Helaby, S. O., Soliman, A. (2004). Solar desalination using humidification–dehumidification processes. part II: an experimental investigation. *Energy Conversion and Management*, 45, 1263–1277.
- [13] Garg, H. P., Adhikari, R. S., Kumar, R. (2002). Experimental design and computer simulation of multi-effect humidification (MEH)-dehumidification solar distillation. *Desalination*, 153, 81-86.
- [14] Ahmed, M. I., Hrairi, M., Ismail, A. F. (2009). On the characteristics of multistage evacuated solar

- distillation. *Renewable Energy*, 34, 1471–1478.
- [15] Parekh, S., Farid, M. M., Selman, J. R., Al-Hallaj, S. (2004). Solar desalination with a humidification-dehumidification technique - a comprehensive technical review. *Desalination*, 160, 167-186.
- [16] Eslamimanesh, A., Hatamipour, M. S. (2010). Economical study of a small-scale direct contact humidification–dehumidification desalination plant. *Desalination*, 250, 203–207.
- [17] TRNSYS Coordinator (2000). A transient system simulation program. Madison. University of Wisconsin,.
- [18] Elsayed, M. M., Taha, I. S., Sabbagh, J. A. (1994). *Design of solar thermal systems*. King Abdulaziz University.
- [19] E1-Nashar, M. (2001). The Economic Feasibility of Small Solar MED Seawater Desalination Plants for Remote Arid Areas. *Desalination*, 134, 173-186.